Beam-based scenario for ^{242m}Am isomer depletion via nuclear excitation by electron capture

J. Rzadkiewicz, M. Polasik, K. Słabkowska, Ł. Syrocki, E. Węder, J. J. Carroll, and C. J. Chiara

Phys. Rev. C **99**, 044309 — Published 18 April 2019

DOI: 10.1103/PhysRevC.99.044309

Beam-based scenario for ^{242m}Am isomer depletion via nuclear excitation by electron capture

J. Rzadkiewicz
National Centre for Nuclear Research, 05-400 Otwock, Poland.

M. Polasik,* K. Słabkowska, Ł. Syrocki, and E. Węder
Faculty of Chemistry, Nicolaus Copernicus University in Toruń, 87-100 Toruń, Poland

J. J. Carroll
U.S. Army Research Laboratory, Adelphi, Maryland 20783, USA

C. J. Chiara
Oak Ridge Associated Universities, U.S. Army Research Laboratory, Adelphi, Maryland 20783, USA
(Dated: April 2, 2019)

Following the first experimental observation of ^{93m}Mo isomer depletion via nuclear excitation by electron capture (NEEC), we consider another experimental scenario related to the ^{242m}Am isomer for which the probability of the NEEC process is expected to be even higher than for the ^{93m}Mo isomer. The optimum experimental conditions for the production and depletion of the ^{242m}Am isomer in a beam-based scenario are discussed. The relevant beam-target reaction cross sections have been calculated striving to ensure effective production of the ^{242m}Am isomer. Kinetic energies required for the NEEC process to occur have been predicted for the n = 5, 6, and 7 subshells of ^{242m}Am ions and combined with available ion charge states at subsequent stages of the ion stopping process. The NEEC resonance strengths have been estimated for the partial contributions of individual subshells to the whole NEEC process.

I. INTRODUCTION

Nuclear isomers, i.e., metastable nuclear excited states, have a unique capacity to store large amounts of energy for an unusually long period of time [1]. Potentially, isomers can be very attractive sources of energy, but in order to use them, one should be able not only to charge such a "nuclear battery", but also release the stored energy on demand (i.e. deplete the isomer) [2, 3]. Several nuclear-excitation mechanisms have been studied in recent years and have been shown to produce depletion for five isomers via photoabsorption, Coulomb-excitation, and thermal neutron capture (see Ref. [4] and references therein). An induction of isomer depletion by Coulomb or photoabsorption excitations is limited by relatively low excitation probabilities and, in addition, in the case of photoabsorption, by the difficulty in matching the energy of an incident photon to the excitation energy from the isomer to an intermediate state whose decay feeds the nuclear ground state [4].

Potentially more effective nuclear-excitation mechanisms involving atomic electrons were also considered for isomer depletion, in particular the process of nuclear excitation by electron capture (NEEC). The concept of NEEC was first introduced outside the isomer depletion idea in Refs. [5, 6] and suggested for possible isomer depletion in Refs. [7–10].

The NEEC process, referred to also as the inverse process of internal conversion, occurs when a free electron is captured into an unfilled atomic shell of an ion and the released energy matches the energy needed for nuclear excitation. Achieving such an energy match is very difficult, because the widths of the excited nuclear states generally are extremely narrow. This was probably one of the main reasons for the inability to observe the NEEC process experimentally for several decades.

Very recently our comprehensive analysis of the optimal atomic conditions for a beam-based experimental scenario [11] has provided crucial guidance for the first observation [12] of isomer depletion via the NEEC process for the long-lived ($T_{1/2}$ = 6.85 h) ^{93m}Mo isomer, at the linear accelerator facility (ATLAS) at Argonne National Laboratory equipped with the Digital Gammasphere [13] γ-ray spectrometer. In this approach, the ^{93}Mo nuclei were produced through the ^{7}Li(^{90}Zr, $p3n$)^{93}Mo fusion-evaporation reaction in inverse kinematics. The experimental observation of NEEC was possible due to careful selection of the ion energy and the thickness of the target layers that, on the one hand, allowed for the efficient production of ^{93}Mo nuclei at high spins and, on the other hand, to enter the ^{93m}Mo ions into the NEEC resonance region with sufficient kinetic energies and charge states.

In earlier studies, it was shown that the NEEC process for a low-lying depletion state (DS) can be the most efficient isomer-depletion mechanism [8], and the NEEC rate should also increase with increasing atomic number Z. For isomeric depletion through $E2$ transitions at low

* Corresponding author: mpolasik@uni.torun.pl

excitation energies, it was predicted that the NEEC process for the ^{242m}Am isomer ($Z = 95$) can be two orders of magnitude more efficient than for the ^{93m}Mo isomer ($Z = 42$) [8].

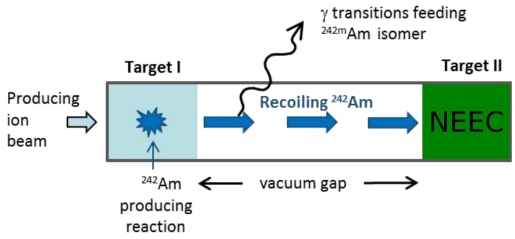

FIG. 1. General scheme for experimental observation of ^{242m}Am isomer depletion via the NEEC process based on Ref. [14]. Not to scale.

Here we discuss the possibility of the production and depletion of the ^{242m}Am isomer in a beam-based experimental scenario. This work is the next step from the first demonstration of NEEC [12] toward a better understanding of the process. We believe that our analysis should also be a significant update of the original proposal presented in Ref. [14]. Figure 1 shows a general scheme for the beam-based ^{242m}Am isomer production and its depletion via NEEC. The scheme is based on the idea of separating (in space and time) three processes: production of ^{242}Am nuclei, feeding of the ^{242m}Am isomeric state from excited recoiling ^{242}Am* ions, and finally providing optimal conditions for NEEC to occur. A suitable detector system would be needed to observe the subsequent signals that NEEC has occurred.

II. ^{242}Am NUCLEI PRODUCTION

The proper choice of the experimental scenario for the beam-based production of ^{242}Am nuclei requires an estimation of the nuclear-reaction cross sections. The relevant cross-sections were calculated by means of the GEMINI++ fusion-evaporation code [15–17]. GEMINI++ is an advanced code based on the statistical decay model describing a complex-fragment formation in fusion-evaporation reactions. The model employs a Monte Carlo simulation technique to predict the decay chains of the compound nuclei (CN) by modes of sequential binary decays. The evaporation of neutrons, protons, and other light particles is treated with the Hauser-Feshbach formalism [18], that takes into account the spin degrees of freedom. Very recently, it was shown that among the codes to calculate fusion-evaporation cross-section, the GEMINI++ gives the most reliable predictions, being typically a factor of 2.8-3.4 too large compared with measured values [19]. More details of the GEMINI++ code can be found in [15–17].

Within the model, the spin (I) distribution for the CN, was assumed to have a roughly triangular shape with a maximum value (I_0) and a cutoff parameter (δI) according to Ref. [16]. In our calculations, we set $\delta I = 2$ and I_0 has been constrained from the Bass model [20]. Fusion reaction parameters used in our study are listed in Table I.

TABLE I. Fusion-evaporation reaction parameters used in the GEMINI++ calculations.

Reaction	CN	CN recoil energy (MeV/nucleon)	Excitation energy (MeV)	Events number
^{242}Pu+^{2}D	^{244}Am	6.1-7.6	20.3-23.2	2×10^5
^{238}U+^{7}Li	^{245}Am	4.6-6.0	33.6-43.8	10^5

Figures 2 and 3 present the cross sections predicted by the GEMINI++ code for the ^{242}Pu+^{2}D and ^{238}U+^{7}Li nuclear reactions leading to the production of ^{242}Am isotopes, among others. In the case of the ^{242}Pu+^{2}D nuclear reaction, the cross section for the ^{242}Am isotope production reaches the maximum for the beam energy of about 6.9 MeV/nucleon. The ^{242}Am isotope production is contaminated by the symmetric fission and the ^{241}Am isotope production. However, for lower beam energy ($E_{beam} < 7$ MeV/nucleon) the contamination can be significantly reduced. The contamination from production of nuclides of other elements is negligible. For ion energies in the range of 6.2-7.0 MeV/nucleon it is still possible to ensure favorable conditions for the NEEC process to take place for n=5, n=6, and n=7 subshells (see the next section).

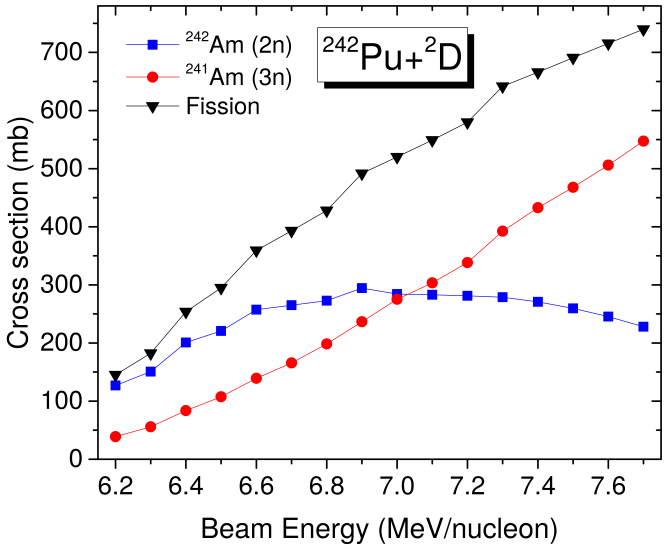

FIG. 2. Cross section for the ^{242}Pu+^{2}D beam-target reaction as a function of the beam energy, calculated with the GEMINI++ code.

Although the production of ^{242}Am isotopes as a result of the ^{238}U + ^{7}Li fusion-evaporation reaction (see

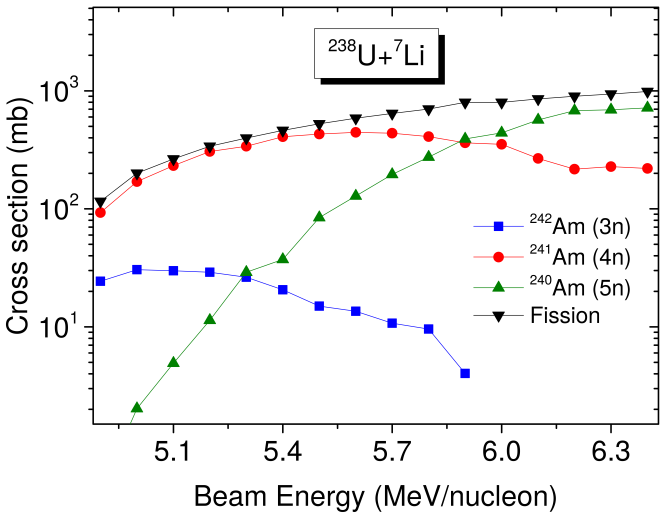

FIG. 3. Cross section (in log scale) for the ^{238}U+^{7}Li beam-target reaction as a function of the beam energy, calculated with the GEMINI++ code.

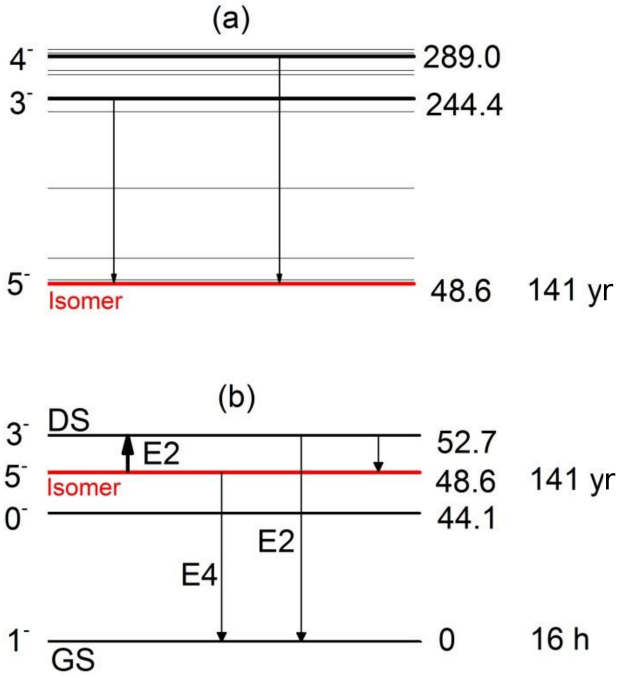

FIG. 4. Partial level scheme (not to scale) for the ^{242}Am nucleus. The level and transition energies given in keV are taken from [21].

Fig. 3) also enables the supply of ions with the necessary high energy required for the NEEC process to occur for n=5, n=6, and n=7 subshells, it is much less effective (i.e., the cross section is lower) in comparison with the ^{242}Pu + ^{2}D reaction. In addition, in the case of the ^{238}U + ^{7}Li reaction, the ^{242}Am isotope production is significantly contaminated by the symmetric fission and by the ^{240}Am and ^{241}Am isotopes (the contamination from other elements is negligible). The only advantage of the ^{238}U + ^{7}Li reaction over the ^{242}Pu + ^{2}D one seems to be technical matters (the higher experimental availability of ^{238}U ions and ^{7}Li target compared to ions of ^{242}Pu and ^{2}D target).

It is worth mentioning that we also analyzed the ^{241}Pu + ^{2}D reaction that was originally proposed in the Ref. [14] for the production of the ^{242}Am isotopes. However, the relevant cross-sections determined for this reaction are significantly smaller than those obtained for nuclear reactions considered above.

The production of the isomeric state ^{242m}Am ($T_{1/2}$ = 141 yr) with the spin $I = 5$ and parity π = -1 ($I^\pi = 5^-$) requires nuclear reactions to lead to a direct formation of the isomer or formation of specific excited states, so that they can efficiently feed the isomer before the ions reach the NEEC conditions region (see Fig. 1). Such low-energy states with $I^\pi = 3^-$ at 244.4 keV and with $I^\pi = 4^-$ at 289.0 keV are shown in Fig. 4(a) which are known to feed the isomer. It is worth mentioning here that the DS at 52.7 keV with $I^\pi = 3^-$ can also feed the isomer, although significant K hindrance is expected for that transition. For NEEC, one should ensure the conditions for the ^{242m}Am isomer depletion through the excitation of the isomeric state with $I^\pi = 5^-$ at 48.6 keV to the DS with $I^\pi = 3^-$ lying 4.1 keV above the isomer that has been observed to decay to the ground state (GS) [see Fig. 4(b)]. The fulfillment of these conditions we discuss in the next section.

III. NEEC ATOMIC RESONANCE CONDITIONS FOR ^{242m}Am ISOMERS IN A BEAM-BASED SCENARIO

After producing ^{242}Am nuclei and feeding the ^{242m}Am isomeric state in the vacuum gap (see Fig. 1), the ^{242m}Am ions should be delivered to the second target in a proper charge state (q) and with a sufficiently high energy required for NEEC. Once the ^{242m}Am ions are delivered to this stopping medium, their energy and ionization degree would decrease systematically as a result of ion-target interactions.

The mean equilibrium charge states (q_{mean}) of the ^{242m}Am ions as a function of the kinetic energy were predicted by means of Schiwietz and Grande formulas [22]. Figure 5 presents this dependence for three stopping media, namely ^{7}Li, ^{12}C and ^{27}Al targets. As can be seen, for C and Al targets, the q_{mean} of the ^{242m}Am ions is slightly lower than for a Li target by ∼0.4 and ∼0.9, respectively. The uncertainties of the q_{mean} obtained from Ref. [22] as a deviation of the experimental values ($\Delta q = \pm 3.0$) from the fit curve for the C solid target is also shown by two dashed red lines.

In order to obtain the values of resonance kinetic energies required for the NEEC process to occur in the case of electron capture into specific atomic subshells for as-

sumed configurations, one has to calculate the appropriate atomic energy levels in ^{242}Am ions. The calculations have been performed for subshells with the main quantum number $5{\leq}n{\leq}7$ and the orbital quantum number l up to l=3 by means of the relativistic, multiconfigurational flexible atomic code (FAC) [23]. The code is based on the modified Dirac-Fock-Slater method that takes into account the Breit and QED corrections. In addition, we verified the obtained values with the multiconfigurational Dirac-Fock (MCDF) method [24–27], which gives almost identical level energies for ^{242}Am ions.

In the calculations, we have used the ground-state configurations for ^{242}Am ions with the charge states from q=+52 to q=+65. For example, for the electron capture into the $5p_{3/2}$ subshell of a ^{242}Am^{+56} ion (Y-like ion) we assumed the [Kr]$4d^3$ initial configuration (before electron capture) and the [Kr]$4d^3 5p_{3/2}$ final configuration (after electron capture). The energy released through electron capture by the ^{242}Am^{+56} ion into the $5p_{3/2}$ subshell obtained as an energy difference of both (initial and final) configurations was found to be 2154.7 eV. This energy requires 3.57 MeV/nucleon kinetic energy of the ^{242m}Am isomer ion for energy matching for the NEEC process. The appropriate value is marked on Fig. 5 as a vertical bar with the height corresponding to the given charge state (q=+56), indicated by specific symbol ($\oplus$) for $5p_{3/2}$ subshell. An analogous method was employed for all other configurations in the respective ion charge states.

Figure 5 presents all potentially possible positions of the ^{242m}Am isomer kinetic energies required for the NEEC process to occur for subshells with $5{\leq}n{\leq}7$ and $0{\leq}l{\leq}3$. The most appropriate kinetic energy positions for the NEEC process may be seen when the bar tops of the subshells, marked as specific symbols, reach the area between the two dashed red lines, describing the q_{mean} deviation values of the ^{242m}Am ion. For each discrete studied charge state q and given shells (n=5, n=6 and n=7) each group of seven bars illustrates, from right to left, electron capture into the $ns_{1/2}$, $np_{1/2}$, $np_{3/2}$, $nd_{3/2}$, $nd_{5/2}$, $nf_{5/2}$, and $nf_{7/2}$ subshells.

One can see that the NEEC process conditions for electron capture into $5s_{1/2}$, $5p_{1/2}$, $5p_{3/2}$, $5d_{3/2}$, $5d_{5/2}$, $5f_{5/2}$, and $5f_{7/2}$ subshells of ^{242m}Am ions can be achieved for charge states from q=+53 up to q=+59 at kinetic energies in a wide range 3.0-4.3 MeV/nucleon (for all stopping media considered in this work). The NEEC process conditions for n=6 subshells ($6s_{1/2}$, $6p_{1/2}$, $6p_{3/2}$, $6d_{3/2}$, $6d_{5/2}$, $6f_{5/2}$ and $6f_{7/2}$) can be accomplished for kinetic energies ranging from ∼4.3 MeV/nucleon up to 5.0 MeV/nucleon for ^{242m}Am with $+57{\leq}q{\leq}+63$, while for n=7 subshells ($7s_{1/2}$, $7p_{1/2}$, $7p_{3/2}$, $7d_{3/2}$, $7d_{5/2}$, $7f_{5/2}$, and $7f_{7/2}$) in a range 5.1-5.7 MeV/nucleon with $+59{\leq}q{\leq}+65$.

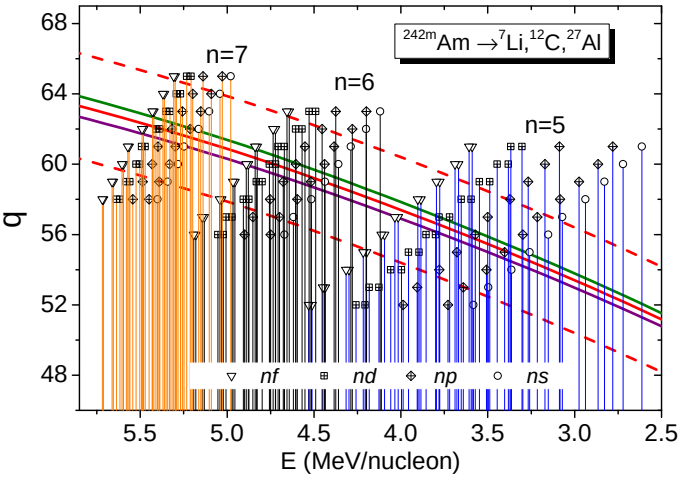

FIG. 5. The q_{mean} of the ^{242m}Am projectile as a function of its kinetic energy for ^{7}Li (green solid line),^{12}C (red solid line) and ^{27}Al (purple solid line) stopping media. The vertical bars present the potential positions of the ^{242m}Am ion NEEC resonance kinetic energy for $ns_{1/2}$, $np_{1/2,3/2}$, $nd_{3/2,5/2}$, and $nf_{5/2,7/2}$ subshells with n=5 (blue bars), n=6 (black bars), and n=7 (orange bars) for the charge states (vertical axis) indicated by specific symbols at the tops of the bars.

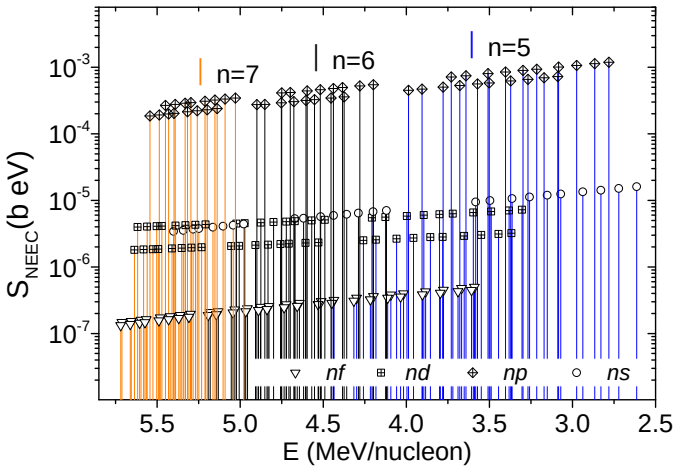

FIG. 6. NEEC resonance strength S^{q,nl_j}_{NEEC} for captures into $ns_{1/2}$, $np_{1/2,3/2}$, $nd_{3/2,5/2}$, and $nf_{5/2,7/2}$ subshells with n=5, n=6, and n=7 for all considered charge states (presented in Fig. 5) plotted as a function of the kinetic energy of ^{242m}Am ions.

IV. NEEC RESONANCE STRENGTH ESTIMATION

Although the NEEC process is formally treated as the reverse process of nuclear internal conversion, the contributions of individual electron orbitals to the NEEC resonance strength may significantly differ from those associated with the internal conversion. This is a result of the dependence of the NEEC resonance strength on the

atomic structure and charge state of an ion.

In order to estimate the NEEC resonance strength for ^{242m}Am isomers for the proposed beam-based scenario with low-Z stopping media, we have applied the approach originally presented in Ref. [28] in which the electron-nuclear interaction is attempted to be described with an accurate treatment. In this approach, the NEEC cross section for the specific charge state q, subshell nl_j at the incident electron energy E is given by

$$\sigma^{q,nl_j}_{NEEC}(E) = S\frac{\pi}{2k^2}\frac{\Gamma^{q,nl_j}_N\Gamma^q_r}{(E-E_r)^2+\frac{1}{4}(\Gamma^q_r)^2}, \qquad (1)$$

where k is the wave number of the incident electron, Γ^{q,nl_j}_N the width of the nuclear transition from the DS to the isomer, and E_r is the energy of the electron for resonant capture. The natural resonance width, Γ^q_r, is the sum of the electronic and nuclear widths. The factor S is a function of the nuclear spins and the total angular momentum of the captured electron [28].

TABLE II. Resonance strength of the NEEC process in ^{242m}Am isomer ($I^\pi = 5^-$) for capture of an electron into nl_j subshells with binding energies (E^{q,nl_j}_b) and for ion kinetic energies (E_k) with charge states q.

q	nl_j	E^{q,nl_j}_b (eV)	α^{q,nl_j}_{IC} (DS $\rightarrow 5^-$)	E_k (MeV/nucleon)	S^{q,nl_j}_{NEEC} (b eV)
+56	$5s_{1/2}$	2383.4	5.3×10^4	3.15	1.2×10^{-5}
+56	$5p_{1/2}$	2304.0	4.2×10^6	3.30	9.0×10^{-4}
+56	$5p_{3/2}$	2154.7	5.8×10^6	3.57	5.6×10^{-4}
+56	$5d_{3/2}$	2030.3	6.8×10^4	3.80	6.2×10^{-6}
+56	$5d_{5/2}$	2000.5	4.6×10^4	3.85	2.8×10^{-6}
+56	$5f_{5/2}$	1870.5	6.6×10^3	4.09	2.8×10^{-7}
+56	$5f_{7/2}$	1860.3	7.9×10^3	4.11	3.4×10^{-7}
+60	$5p_{1/2}$	2539.3	4.6×10^6	2.87	1.1×10^{-3}
+60	$5p_{3/2}$	2373.2	5.8×10^6	3.17	7.0×10^{-4}
+83	$5p_{3/2}$	3964.3	-	-	3.6×10^{-3} [a]
+60	$6p_{1/2}$	1682.6	3.1×10^6	4.44	4.8×10^{-4}
+60	$6p_{3/2}$	1592.6	4.3×10^6	4.60	3.2×10^{-4}
+60	$7p_{1/2}$	1196.5	2.2×10^6	5.33	2.9×10^{-4}
+60	$7p_{3/2}$	1142.4	3.1×10^6	5.43	2.0×10^{-4}

[a] Value published in Ref. [8]

In order to obtain the resonance strength of the NEEC process for a given atomic state, one has to integrate the cross section over the relative energy of the captured electron

$$S^{q,nl_j}_{NEEC} = \int \sigma^{q,nl_j}_{NEEC}(E)dE. \qquad (2)$$

Finally, the resonance strength of the NEEC process for the ^{242m}Am isomer ($I^\pi = 5^-$) takes the modified version of the form presented in Ref. [7]

$$S^{q,nl_j}_{NEEC} = S\frac{\lambda_e^2}{4}\frac{\alpha^{q,nl_j}_{IC}(\mathrm{DS}\rightarrow 5^-)\Gamma_\gamma(\mathrm{DS}\rightarrow 5^-)}{\Gamma_t(\mathrm{DS})} \times(1+\alpha^{q=0}_{IC}(\mathrm{DS}\rightarrow \mathrm{GS}))\Gamma_\gamma(\mathrm{DS}\rightarrow \mathrm{GS}), \qquad (3)$$

where λ_e is the wavelength of the capture electrons with the relative kinetic energy required for NEEC to occur, $\alpha^{q,nl_j}_{IC}(\mathrm{DS}\rightarrow 5^-)$ is the internal-conversion coefficient (ICC) for the nl_j subshell and charge state q, $\Gamma_\gamma(\mathrm{DS}\rightarrow 5^-)$ and $\Gamma_\gamma(\mathrm{DS}\rightarrow \mathrm{GS})$ are radiative transition widths and $\Gamma_t(\mathrm{DS})$ the total width of the DS ($I^\pi = 3^-$). The total ICC, $\alpha^{q=0}_{IC}(\mathrm{DS}\rightarrow \mathrm{GS})$, is the sum of partial coefficients determined for all subshells in neutral ^{242}Am atom. This assumption is due to the fact that the (DS $\rightarrow$ GS) transition is delayed in time with respect to the NEEC process and therefore occurs in the ^{242}Am ions with lower charge states in comparison to those during the NEEC process. Moreover, the main contribution to the total ICC comes from the L- and M-subshells, whose partial ICCs are less sensitive to ionization of the outer atomic shells than the subshells with n=5, n=6, and n=7. The reduced transition probabilities of the DS and the corresponding nuclear level width were calculated by means of Weisskopf single-particle estimations [29]. As was shown by Pálffy *et al.*, the use of appropriate values of ICCs is crucial in that kind of calculation [8]. The use of inappropriate ICCs led to an underestimation of the NEEC strengths by many orders of magnitude in Ref. [7].

In our estimations, the ICCs were calculated by the so called *Frozen Orbital* (FO) approximation based on the Dirac-Fock calculations taking into account the effect of atomic vacancies created in the conversion process. In this approximation, the electron wave functions of the initial and final states are calculated in the self-consistent field (SCF) of a neutral atom (q=0) and in the ion potential constructed using bound wave functions of the neutral atom, respectively. It was shown that the ICC predictions based on the Dirac-Fock calculations are able to reproduce the experimental values at high level of accuracy (with uncertainty less than 1%) for a neutral atom (for details see Refs. [30, 31]). In order to modify the ICC for neutral atoms into the coefficients for highly ionized ^{242m}Am ions (up to q=+65) we assumed the linear scaling dependence

$$\frac{\alpha^{q,nl_j}_{IC}(\mathrm{DS}\rightarrow 5^-)}{E^{q,nl_j}_b} = \frac{\alpha^{q=0,nl_j}_{IC}(\mathrm{DS}\rightarrow 5^-)}{E^{q=0,nl_j}_b}, \qquad (4)$$

where $\alpha^{q,nl_j}_{IC}(\mathrm{DS}\rightarrow 5^-)$, $\alpha^{q=0,nl_j}_{IC}(\mathrm{DS}\rightarrow 5^-)$ and E^{q,nl_j}_b, $E^{q=0,nl_j}_b$ are ICCs and binding energies of a specific subshell nl_j for highly ionized ions and neutral atoms, respectively. The binding energies for neutral atoms were

taken from tables [32], while those for highly ionized ions were calculated by us (see Section III). The accuracy of the ICCs estimated by us for Am ions would be worse than for neutral atoms, because of the linear scaling procedure imperfection (<5%) and uncertainty of the atomic binding energy calculations (<1%). However, the evaluation of total ICCs uncertainties and their influence on the final uncertainties of the NEEC strengths would require an experimental verification. It is worth mentioning here that the NEEC strength derived from the $\alpha_{IC}^{q,nl_j}(\mathrm{DS} \rightarrow 5^-)$ is proportional to the real number of vacancies available for NEEC in a specific subshell of the ^{242m}Am ion. Conversely, in the internal conversion process ICCs are proportional to the number of electrons in a given subshell and not the number of vacancies.

Figure 6 shows resonance strengths of the NEEC process in ^{242m}Am ions for all n=5, n=6, and n=7 (l up to 3) subshells and charge states corresponding to those presented in Fig. 5. The NEEC processes into subshells with n<5 are not considered because they are generally energetically forbidden. Table II shows, in addition, numerical values of the NEEC resonance strengths for selected subshells and charge states that can appear in subsequent resonances during stopping of ^{242m}Am ions in the low-Z solid targets. The highest partial contributions to the NEEC process in the beam-based scenario come from captures into $np_{1/2}$ and $np_{3/2}$ subshells, in particular into $5p_{1/2}$ and $5p_{3/2}$.

One can see in Fig. 6 that, for each considered subshell, NEEC resonance strengths systematically increase with decreasing kinetic energy of ^{242m}Am ions as a result of the increase of binding energy for ions in higher charge states (see Table II). In Fig. 6 all np values of resonance strengths are represented by the highest vertical bars in the range from $\sim 2\times10^{-4}$ b eV (for capture into $7p$ subshells of $^{242m}\mathrm{Am}^{+58}$ at ∼5.5 MeV/nucleon kinetic energy) to $\sim 1\times10^{-3}$ b eV (for capture into $5p$ subshells of $^{242m}\mathrm{Am}^{+61}$ at ∼2.8 MeV/nucleon kinetic energy). It is worth noting here that the values of resonance strengths estimated by us for the $5p_{3/2}$ subshell are over 13 orders of magnitude larger than the values obtained in Ref. [7]. Our estimated values for the $5p_{3/2}$ subshell at the highest considered charge states approach the value of 3.6×10^{-3} b eV obtained for $^{242m}\mathrm{Am}^{+83}$ by Pálffy *et al.*, from the advanced theory based on a Feshbach projection operator formalism [8].

Partial contributions to the NEEC process originating from captures into ns and nd subshells are more than an order of magnitude lower than those from np ones. The weakest NEEC resonance strengths (not exceeding the value of 5×10^{-7} b eV) were obtained for nf subshells.

To ensure optimal conditions for the occurrence of the NEEC process in the beam-based scenario, the resonance strengths of ^{242m}Am ions must be combined with the available high charge states, the number of which is significantly limited at low kinetic energies (see Fig. 5). On the basis of Figs. 5 and 6, and Table II, it has been found that the most efficient atomic conditions for the NEEC process to occur are for the $5p_{1/2}$ and $5p_{3/2}$ subshells of ^{242m}Am ions with q=+55 and q=+56 at kinetic energies of 3.3-3.4 MeV/nucleon. Slightly less but still very efficient conditions occur for the NEEC process in ^{242m}Am ions at the kinetic energies of 4.6-4.7 MeV/nucleon and for captures into $6p_{1/2}$ and $6p_{3/2}$ subshells for q=+59 and q=+60. High contributions to NEEC from captures into $7p_{1/2}$ and $7p_{3/2}$ subshells for the high charge states (q ∼+62) at the kinetic energies of ∼5.3 MeV/nucleon are also available. That is a result of the high beam-energy requirement (∼7.0 MeV/nucleon) necessary for efficient production of ^{242}Am nuclei, especially for the ^{242}Pu + ^{2}D beam-target reaction (see Fig. 2).

V. SUMMARY AND CONCLUSIONS

The beam-based scenario for the production and depletion of the ^{242m}Am isomer ($T_{1/2}$ = 141 yr, $I^\pi = 5^-$) through its excitation to the 52.7-keV level ($I^\pi = 3^-$) by electron capture has been considered. The cross sections calculated by means of the GEMINI++ fusion-evaporation code indicate that the ^{242}Pu+^{2}D nuclear reaction can be used for the efficient production of ^{242}Am isotopes, especially at high beam energy (∼7.0 MeV/nucleon). The production is also possible in the ^{238}U+^{7}Li nuclear reaction but less efficiently. It was also shown that the ^{242}Am nuclide production can be contaminated by the symmetric fission and production of other Am isotopes. The contamination from other elements is negligible.

The necessary kinetic energies required for the NEEC process to occur have been predicted for n=5, 6, and 7 subshells of ^{242m}Am ions in various charge states expected in subsequent stages of the ion-stopping process. The NEEC resonance strengths have been estimated in order to recognize the partial contributions to the whole NEEC process from the specific atomic subshells.

Further, it was shown that the highest partial contributions to the NEEC process in the beam-based scenario should come from captures into $5p$ and $6p$ subshells of ^{242m}Am ions with charge states from q≈+54 to q≈+62 at kinetic energies of 3.0-5.0 MeV/nucleon. High partial contributions to NEEC from captures into $7p$ subshells at the kinetic energies above ∼5 MeV/nucleon are also available due to the high beam energy requirement needed to obtain the largest possible cross sections for the ^{242}Am isotope production, especially for the ^{242}Pu+^{2}D beam-target reaction. Electron captures into ns and nd subshells should give much smaller contributions to the NEEC process in comparison with np ones, while captures into nf subshells seem to be negligible.

ACKNOWLEDGMENTS

This work is supported by the National Science Centre, Poland under grant number 2017/25/B/ST2/00901 and by the US Army Research Laboratory under Cooperative Agreement Number W911NF-16-2-0034.

[1] P. Walker and G. Dracoulis, Nature **399**, 35 (1999).
[2] H. Roberts, Hyperfine Interact. **107**, 91 (1997).
[3] J. J. Carroll, 'Nuclear Metastables for Energy and Power: Status and Challenges', in *Innovations in Army Energy and Power Materials Technologies*, edited by E. C. Shaffer and T. S. Zheleva (Materials Research Forum, Millersville, PA, 2018).
[4] J. J. Carroll *et al.*, AIP Conf. Proc. **1525**, 586 (2013).
[5] V. I. Goldanskii and V. A. Namiot, Phys. Lett. B **62**, 393 (1976).
[6] N. Cue, J.-C. Poizat, and J. Remillieux, Europhys. Lett. **8**, 19 (1989).
[7] A. A. Zadernovsky and J. J. Carroll, Hyperfine Interact. **143**, 153 (2002).
[8] A. Pálffy, J. Evers, and C. H. Keitel, Phys. Rev. Lett. **99**, 172502 (2007).
[9] J. Gunst, Y. A. Litvinov, C. H. Keitel, and A. Pálffy, Phys. Rev. Lett. **112**, 082501 (2014).
[10] Y. Wu, J. Gunst, C. H. Keitel, and A. Pálffy, Phys. Rev. Lett. **120**, 052504 (2018).
[11] M. Polasik, K. Słabkowska, J. J. Carroll, C. J. Chiara, Ł. Syrocki, E. Węder, and J. Rzadkiewicz, Phys. Rev. C **95**, 034312 (2017).
[12] C. J. Chiara, J. J. Carroll, M. P. Carpenter, J. P. Greene, D. J. Hartley, R. V. F. Janssens, G. J. Lane, J. C. Marsh, D. A. Matters, M. Polasik, J. Rzadkiewicz, D. Seweryniak, S. Zhu, S. Bottoni, A. B. Hayes, and S. A. Karamian, Nature **554**, 216 (2018).
[13] J. T. Anderson *et al.*, 2012 IEEE Nucl. Sci. Symp. Med. Imaging Conf. **N20-2**, 1536 (2012).
[14] S. A. Karamian and J. J. Carroll, Phys. At. Nucl. **75**, 1362 (2012).
[15] R. J. Charity *et al.*, Nucl. Phys. A **483**, 371 (1988).
[16] R. J. Charity, Phys. Rev. C **82**, 014610 (2010).
[17] D. Mancusi, R. J. Charity, and J. Cugnon, Phys. Rev. C **82**, 044610 (2010).
[18] W. Hauser and H. Feshbach, Phys. Rev. **87**, 366 (1952).
[19] B. Blank, G. Canchel, F. Seis, and P. Delahaye, Nucl. Instrum. Methods Phys. Res. B **416**, 41 (2018).
[20] R. Bass, Nucl. Phys. A **231**, 45 (1974); Phys. Rev. Lett. **39**, 265 (1977).
[21] Y. A. Akovali, Nucl. Data Sheets **96**, 177 (2002).
[22] G. Schiwietz and P. L. Grande, Nucl. Instrum. Methods Phys. Res. B **175-177**, 125 (2001).
[23] M. F. Gu, Can. J. Phys. **86**, 675 (2008).
[24] I. P. Grant and H. M. Quiney, Adv. At. Mol. Phys. **23**, 37 (1988).
[25] K. G. Dyall, I. P. Grant, C. T. Johnson, F. A. Parpia, and E. P. Plummer, Comput. Phys. Commun. **55**, 425 (1989).
[26] M. Polasik, Phys. Rev. A **39**, 616 (1989); **39**, 5092 (1989); **40**, 4361 (1989); **41**, 3689 (1990); **52**, 227 (1995).
[27] M. Polasik, K. Słabkowska, J. Rzadkiewicz, K. Kozioł, J. Starosta, E. Wiatrowska-Kozioł, J.-Cl. Dousse, and J. Hoszowska, Phys. Rev. Lett. **107**, 073001 (2011).
[28] M. R. Harston and J. F. Chemin, Phys. Rev. C **59**, 2462 (1999).
[29] P. Ring and P. Schuck, *The Nuclear Many-Body Problem* (Springer-Verlag, New York, 1980).
[30] S. Raman, C. W. Nestor Jr., A. Ichihara, and M. B. Trzhaskovskaya, Phys. Rev. C **66**, 044312 (2002).
[31] T. Kibédi, T. W. Burrows, M. B. Trzhaskovskaya, P. M. Davidson, and C. W. Nestor Jr., Nucl. Instrum. Methods Phys. Res. A **589**, 202 (2008).
[32] F. B. Larkins, At. Data and Nucl. Data Tables **20**, 313 (1977).